

Supporting Information

Mg(I)-Fe(-II) and Mg(0)-Mg(I) Covalent Bonding in the $Mg_nFe(CO)_4^-$ ($n = 1, 2$) Anion Complexes: An Infrared Photodissociation Spectroscopic and Theoretical Study

Xiaoyang Jin, Guanjun Wang, Mingfei Zhou*

Collaborative Innovation Center of Chemistry for Energy Materials, Department of Chemistry, Shanghai Key Laboratory of Molecular Catalysis and Innovative Materials, Fudan University Shanghai 200438 (China). E-mail: mfzhou@fudan.edu.cn

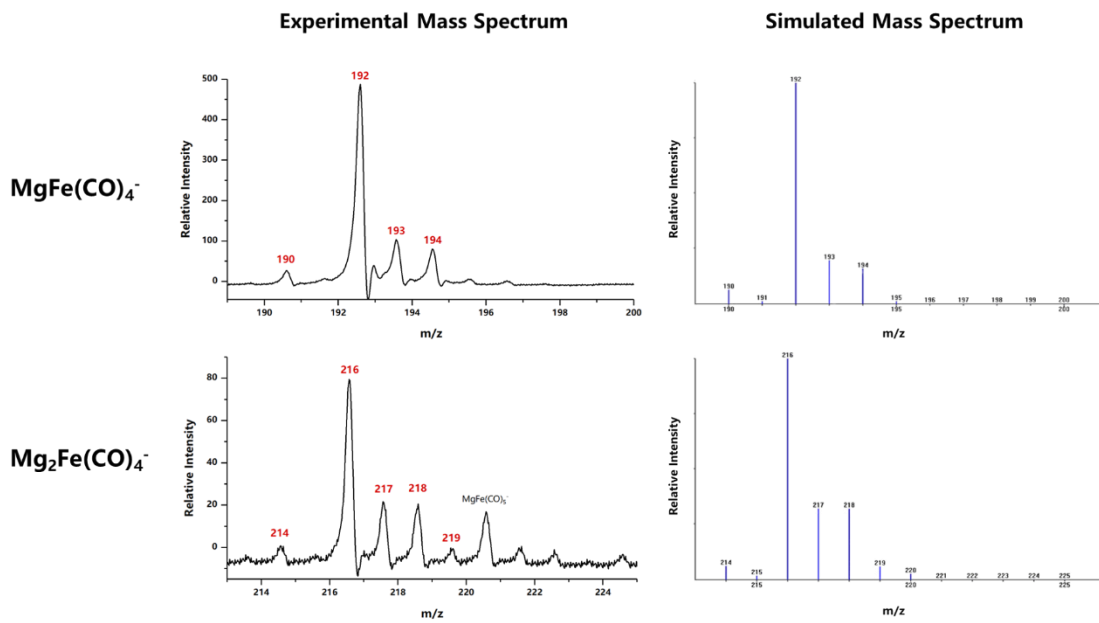


Figure S1. The experimental mass spectra of $\text{MgFe}(\text{CO})_4^-$ and $\text{Mg}_2\text{Fe}(\text{CO})_4^-$ and the corresponding simulated mass spectra based on natural isotope abundances of the elements. The number of Mg atoms can be confirmed according to the isotopic splitting.

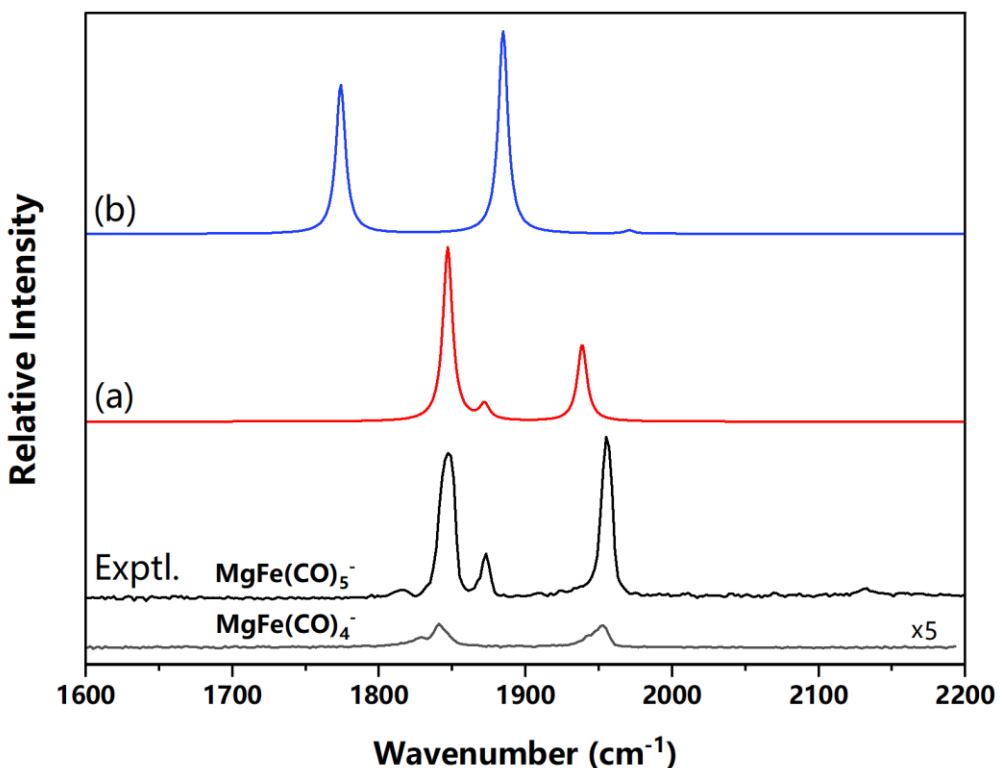


Figure S2. The experimental IR spectra of $\text{MgFe}(\text{CO})_4^-$ and $\text{MgFe}(\text{CO})_5^-$ and the simulated IR spectra of the two lowest-lying isomers (as shown in Table S1) of $\text{MgFe}(\text{CO})_4^-$ at the B3LYP/aug-cc-pVTZ level. The predicted IR spectra were obtained from scaled harmonic vibrational frequencies for the two isomers of $\text{MgFe}(\text{CO})_4^-$ by applying Lorentzian line shape function with 4 cm⁻¹ full-width-at-half-maximum.

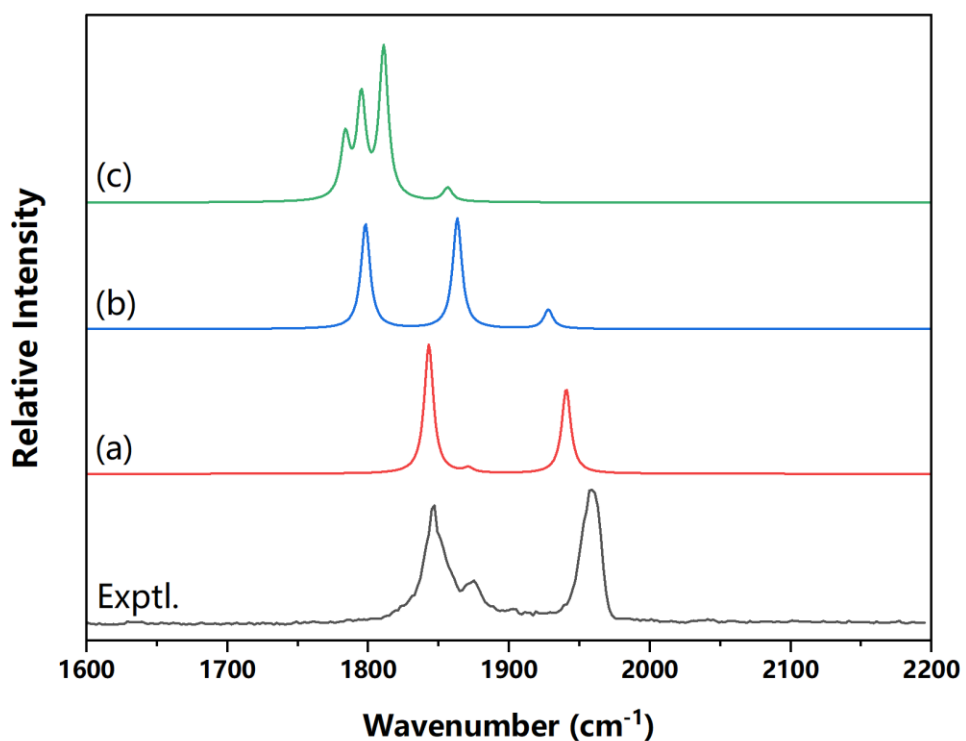


Figure S3. The experimental IR spectrum and the simulated IR spectra of the three lowest-lying isomers (as shown in Table S2) of $\text{Mg}_2\text{Fe}(\text{CO})_4^-$ at the B3LYP/aug-cc-pVTZ level. The predicted IR spectra were obtained from scaled harmonic vibrational frequencies for the three isomers of $\text{Mg}_2\text{Fe}(\text{CO})_4^-$ by applying Lorentzian line shape function with 4 cm^{-1} full-width-at-half-maximum.

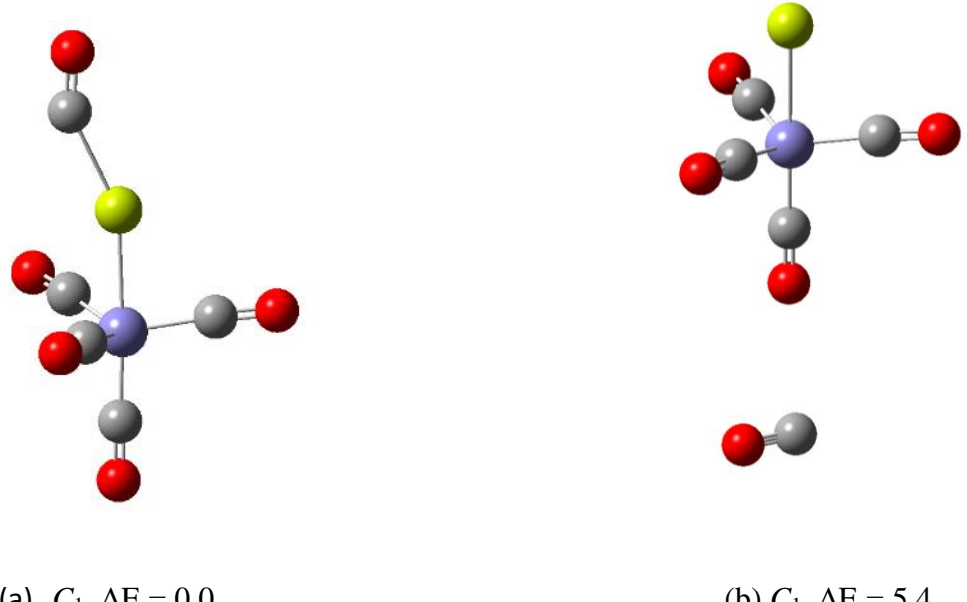


Figure S4. Optimized equilibrium geometries and relative energies ($\text{kcal}\cdot\text{mol}^{-1}$) of different isomers of $\text{MgFe}(\text{CO})_5^-$ in the doublet spin state at the B3LYP/aug-cc-pVTZ level of theory. Color codes for atoms: red, O; gray, C; purple, Fe; green, Mg.

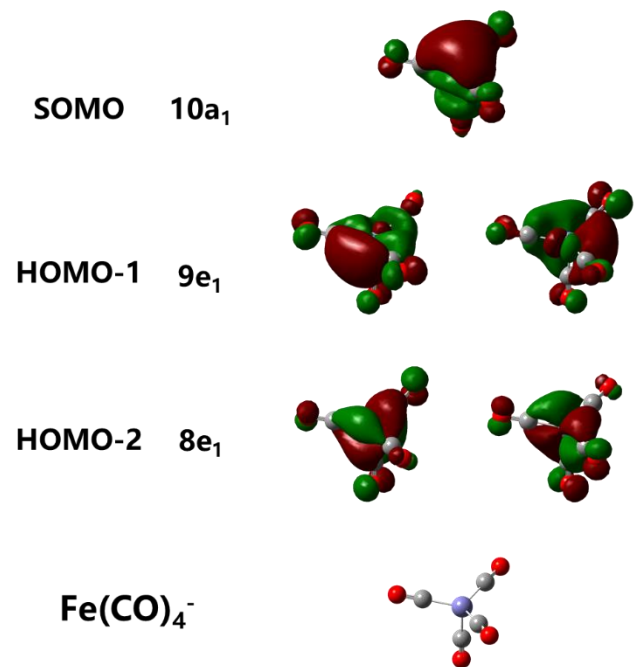


Figure S5. The contours of the frontier Kohn-Sham canonical valence MOs of the 2A_1 - $\text{Fe}(\text{CO})_4^-$ at the B3LYP/aug-cc-pVTZ level (isosurface = 0.03 au.). Color codes for atoms: red, O; gray, C; purple, Fe.

Table S1. Calculated geometries and relative energies (kcal·mol⁻¹) of different isomers of MgFe(CO)₄⁻ in the doublet spin state at the B3LYP/aug-cc-pVTZ level of theory. Color codes for atoms: red, O; gray, C; purple, Fe; green, Mg.

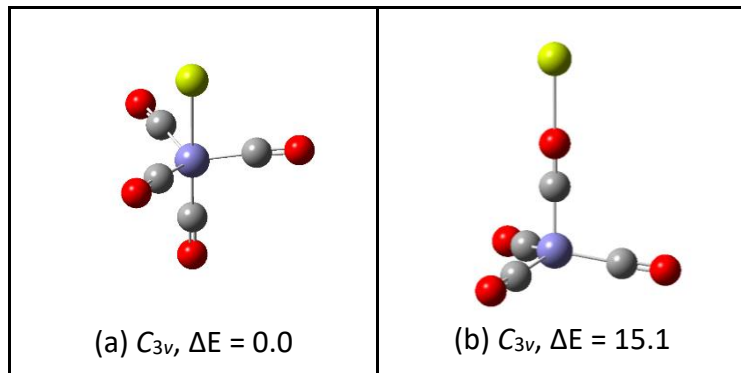


Table S2. Calculated geometries and relative energies (kcal·mol⁻¹) of different isomers of Mg₂Fe(CO)₄⁻ in the doublet spin state at the B3LYP/aug-cc-pVTZ level of theory. Color codes for atoms: red, O; gray, C; purple, Fe; green, Mg.

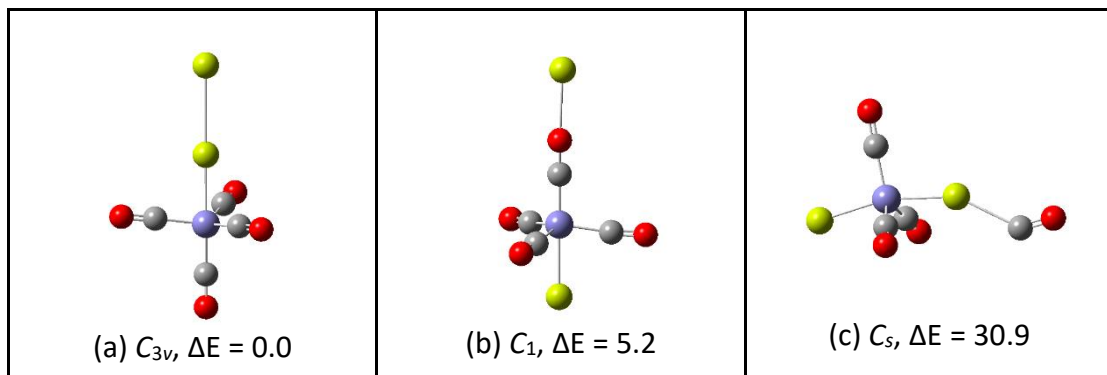


Table S3. Calculated bond dissociation energies D_0 (kcal·mol⁻¹) of MgFe(CO)₄⁻, MgFe(CO)₅⁻ and Mg₂Fe(CO)₄⁻ for the loss of one magnesium atom or one carbon monoxide (the axial CO for MgFe(CO)₄⁻ and Mg₂Fe(CO)₄⁻ and the tagging CO for MgFe(CO)₅⁻) at the B3LYP/aug-cc-pVTZ level of theory.

	D_0 (-Mg)	D_0 (-CO)
MgFe(CO) ₄ ⁻	18.3	40.9
MgFe(CO) ₅ ⁻	18.2	0.7
Mg ₂ Fe(CO) ₄ ⁻	2.5	39.9

Table S4. Charge analyses of ${}^2\text{A}_1$ -MgFe(CO)₄⁻ with Hirshfeld, VDD, QTAIM and NPA at the B3LYP/aug-cc-pVTZ level.

Atom	Spin density	Hirshfeld	VDD	AIM	NPA
Mg	0.55	0.04	0.04	0.52	0.47
Fe	0.42	-0.20	-0.21	0.36	-2.38
C	0.00	0.00	0.01	0.73	0.76
C	0.00	0.00	0.01	0.73	0.76
C	0.00	0.00	0.01	0.73	0.76
O	0.00	-0.22	-0.23	-1.24	-0.57
O	0.00	-0.22	-0.23	-1.24	-0.57
O	0.00	-0.22	-0.23	-1.24	-0.57
C	0.07	0.04	0.06	0.89	0.87
O	-0.02	-0.20	-0.22	-1.23	-0.55

Table S5. Charge analyses of ${}^2\text{A}_1$ - $\text{Mg}_2\text{Fe}(\text{CO})_4^-$ with Hirshfeld, VDD, QTAIM and NPA at the B3LYP/aug-cc-pVTZ level.

Atom	Spin density	Hirshfeld	VDD	AIM	NPA
Mg11 ^[a]	0.31	-0.17	-0.17	-0.11	-0.02
Mg8 ^[a]	0.22	0.22	0.22	0.69	0.49
Fe	0.48	-0.20	-0.22	0.32	-2.41
C	-0.01	-0.01	0.01	0.71	0.77
C	-0.01	-0.01	0.00	0.72	0.77
C	-0.01	-0.01	0.00	0.72	0.77
O	0.00	-0.22	-0.23	-1.24	-0.56
O	0.00	-0.22	-0.23	-1.24	-0.56
O	0.00	-0.22	-0.23	-1.24	-0.56
C	0.05	0.04	0.06	0.88	0.88
O	-0.02	-0.20	-0.22	-1.21	-0.55

[a] The number is referred to the atom label in Figure 3.

Table S6. AO contributions (in %) in Kohn-Sham MOs of ${}^2\text{A}_1\text{-MgFe}(\text{CO})_4^-$ at the B3LYP/aug-cc-pVTZ level of theory.

		Mg		Fe		CO	
		3s	3p	4s	3d	4p	2s2p
SOMO 11a ₁	α	45.9	19.0	0.7	13.7	6.9	11.4
HOMO 9e ₁	α		1.3		48.7	12.7	35.1
	β		1.2		48.0	12.6	36.0
HOMO-1 10a ₁	α	34.7	0.1	0.3	24.4	14.1	23.2
	β	33.9	0.1	0.5	24.6	14.9	23.7
HOMO-2 8e ₁	α				80.2		19.1
	β				79.1		20.2

Table S7. AO contributions (in %) in Kohn-Sham MOs of ${}^2\text{A}_1\text{-Mg}_2\text{Fe}(\text{CO})_4^-$ at the B3LYP/aug-cc-pVTZ level of theory.

	α	Mg8 ^[a]		Mg11 ^[a]		4s	3d	4p	CO 2s2p
		3s	3p	3s	3p				
SOMO 12a ₁	α	26.8	12.3	15.8	23.6	0.3	8.1	4.3	6.3
HOMO 9e ₁	α		1.8				48.1	12.5	35.5
	β		1.7				47.7	12.5	36.0
HOMO-1 11a ₁	α	4.8	1.5	31.3	0.9	0.5	24.1	13.7	21.2
	β	5.2	2.8	31.6		0.5	23.3	13.6	20.9
HOMO-2 8e ₁	α						79.7		19.6
	β		0.1				79.0		20.3
HOMO-3 10a ₁	α	30.6	6.4	46.9	0.6		4.9	2.7	6.0
	β	27.7	5.1	48.4	1.1		5.8	3.4	6.7

[a] The number is referred to the atom label in Figure 3.

Table S8. The deformation densities $\Delta\rho$ (red → blue, isosurface = 0.001 au.) of ${}^2\text{A}_1$ -MgFe(CO)₄⁻ using Mg in the ${}^3\text{P}$ ($3\text{s}^13\text{p}^1$) excited state and Fe(CO)₄⁻ in the ${}^2\text{A}_1$ ground state as interaction fragments based on the EDA-NOCV analysis at the PBE/TZ2P level. Energy values are given in kcal·mol⁻¹. The value in parentheses gives the percentage contribution to the total orbital interactions ΔE_{orb} .

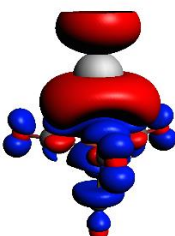
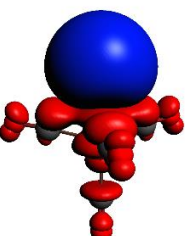
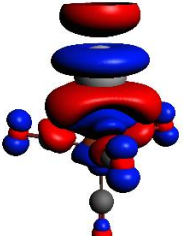
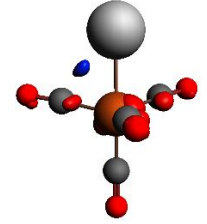
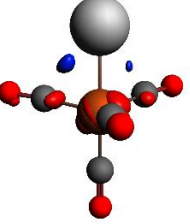
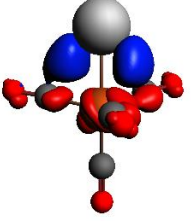
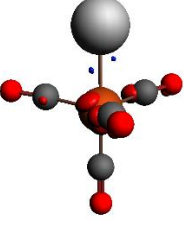
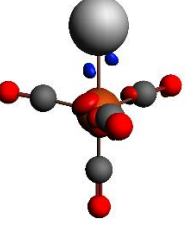
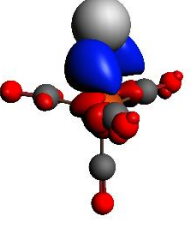
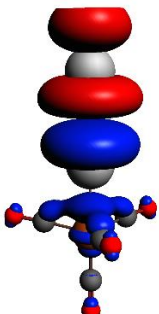
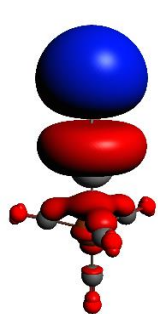
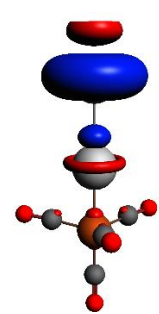
Fragment	Mg: $3\text{s}^13\text{p}^1$ Fe(CO) ₄ ⁻ : ${}^2\text{A}_1$		
	α	β	$\alpha+\beta$
$\Delta E_{\text{orb}(\sigma)}$	 $\Delta E_{\sigma\alpha} = -76.3$ $ v_{\sigma\alpha} = 0.75$	 $\Delta E_{\sigma\beta} = -15.1$ $ v_{\sigma\beta} = 0.47$	 $\Delta E_{\sigma} = -91.4$ (88.9%) $ v_{\sigma} = 0.28$
$\Delta E_{\text{orb}(\pi_1)}$	 $\Delta E_{\pi_1\alpha} = -2.3$ $ v_{\pi_1\alpha} = 0.11$	 $\Delta E_{\pi_1\beta} = -1.8$ $ v_{\pi_1\beta} = 0.11$	 $\Delta E_{\pi_1} = -4.1$ (4.0%) $ v_{\pi_1} = 0.22$
$\Delta E_{\text{orb}(\pi_2)}$	 $\Delta E_{\pi_2\alpha} = -2.3$ $ v_{\pi_2\alpha} = 0.11$	 $\Delta E_{\pi_2\beta} = -1.8$ $ v_{\pi_2\beta} = 0.11$	 $\Delta E_{\pi_2} = -4.1$ (4.0%) $ v_{\pi_2} = 0.22$
$\Delta E_{\text{orb}(\text{rest})}$	-1.9	-1.3	-3.2 (3.1%)

Table S9. The deformation densities $\Delta\rho$ (red → blue, isosurface = 0.001 au.) of ${}^2\text{A}_1\text{-Mg}_2\text{Fe}(\text{CO})_4^-$ using Mg in the ${}^3\text{P}$ ($3s^13p^1$) excited state and $\text{MgFe}(\text{CO})_4^-$ in the ${}^2\text{A}_1$ ground state as interaction fragments based on the EDA-NOCV analysis at the PBE/TZ2P level. Energy values are given in $\text{kcal}\cdot\text{mol}^{-1}$. The value in parentheses gives the percentage contribution to the total orbital interactions ΔE_{orb} .

Fragment	Mg: $3s^13p^1$ $\text{MgFe}(\text{CO})_4^-: {}^2\text{A}_1$		
	α	β	$\alpha+\beta$
$\Delta E_{\text{orb}(\sigma)}$	 $\Delta E_{\sigma\alpha} = -15.9$ $ v_{\sigma\alpha} = 0.53$	 $\Delta E_{\sigma\beta} = -32.9$ $ v_{\sigma\beta} = 0.70$	 $\Delta E_{\sigma} = -48.8 \text{ (95.3\%)}$ $ v_{\sigma} = 0.17$
$\Delta E_{\text{orb}(\text{rest})}$	-1.3	-1.1	-2.4 (4.7%)